Image-Processing-Based State Estimation for Vehicle Lateral Control using Multi-rate Kalman Filter

Yafei Wang[*,1], Binh Minh Nguyen[1], Palakon Kotchapansompote[1], Hiroshi Fujimoto[2] and Yoichi Hori[2]

[1]*Department of Electrical Engineering, Graduate School of Engineering, The University of Tokyo, Tokyo, 113-0033, Japan*
[2]*Department of Advanced Energy, Graduate School of Frontier Sciences, The University of Tokyo, Chiba, 227-8561, Japan*
Received: ---; Revised: ----; Accepted: ---

Abstract: Driver assistance systems such as automatic steering for lane keeping are of particular importance for vehicle's lateral safety; on the other hand, vehicle states such as relative lateral position to lane, orientation, and lateral velocity are key enablers for realization of the above mentioned applications. To obtain the lane information for lateral control, look-ahead cameras are widely employed, and lots of papers and patents on vision-based lane keeping have been generated in the past few decades. Nevertheless, the sampling rate of normal camera is 30 Hz which is much slower compared with other kinds of onboard sensors/actuators, and the time delay caused by image processing is too long to be neglected. Previous researches and patents simply adapt the whole system's sampling frequency to the lowest one; however, the held and delayed feedbacks deteriorate system performances and even cause instability. Here, the two problems are solved using a multi-rate Kalman filter (KF) with measurement delays included, and the open loop stability margin is increased accordingly. In this paper, first of all, vehicle and visual models are explained followed with experimental setup introduction; then, real-time image processing algorithms are briefly introduced; and then, multi-rate Kalman filter considering time delay is designed for vehicle states estimation; then, the proposed method is verified with both simulations and experiments; finally, conclusion, current and future developments are presented.

Keywords: Lane detection, measurement delay, multi-rate Kalman filter, sensor fusion, vehicle lateral control, vision system.

1. INTRODUCTION

With the increasing concern for highway safety and automation, driver assistance systems, for example, automatic steering devices for lane keeping, have been extensively investigated by automotive companies and research institutions. Joel C. McCall *et al.* surveyed some previous researches, proposed their own methods for lane detection and evaluated the methods with systematic criterions [1]; another research was conducted by M. Bertozzi *et al.* [2], they used stereo vision system to detect lane and obstacles on the road. In addition to the literatures in academic field, many patents were generated on lane detection and lane following systems. Timothy W. Kaufmann *et al.* proposed methods to detect vehicle offset to the lane and to control steering wheel accordingly for lane keeping [3]; Toru Saito *et al.* invented a similar device for lane keeping assistance [4]. While lane keeping strategies of these proposed methods differ somehow, most of them use cameras and image processing system for lane detection and location. However, problems arise with the utilization of normal cameras in three aspects:

1) As is well-known, the sampling rate of normal cameras is 30 Hz, and this is not fast enough for vehicle motion control applications [14]. In [5], differential braking realized by brake-by-wire system is used for vehicle lateral control and yaw stability control. Vehicles with other kinds of driving structure such as in-wheel-motor vehicle can generate differential torque more quickly and precisely [6-7]; in this case, the multi-rate ratio between input and output becomes even bigger.
2) Most of the onboard sensors work at 1 kHz which are much faster than that of normal cameras; therefore, they can not be fused directly. Although high-speed cameras have already been commercialized, the cost is too high to be practically employed for automotive applications.
3) Image processing takes time and brings delay into the outputs; this delay generally cannot be neglected.

For the problems above, most previous researches and patents simply neglect the multi-rate issue, i.e., vehicle states are updated at the sampling rate of camera; some of them ignore the delay caused by image processing. However, the held and delayed feedbacks deteriorate system performance and even cause instability. If the updating rate of vehicle state estimator can be boosted, the performances of vehicle lateral control can be enhanced accordingly. Vehicle's relative position to lane, orientation and lateral velocity are the main states for vehicle lateral control, and they are difficult to be obtained directly; estimation methods hence need to be developed.

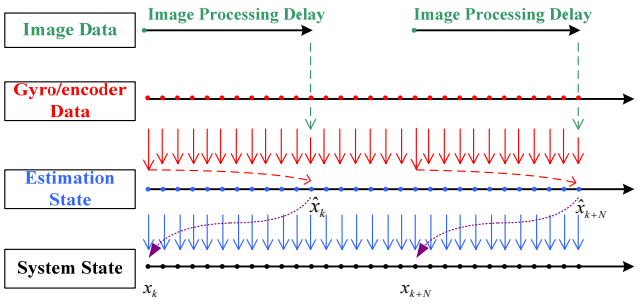

Fig. (1). System sampling sequence.

*Address Correspondence to this author at the Department of Electrical Engineering, Graduate School of Engineering, The University of Tokyo, Tokyo, 113-0033, Japan; Tel: +81-04-7136-3873, Fax: +81-04-7136-3847; E-mail: wang@hori.k.u-tokyo.ac.jp

2210-6863/11 $100.00+.00

In this study, a combined vehicle and vision system is modeled. The model has four states and three of them can be obtained from sensor/image processing program. The vehicle model is based on bicycle model which is also known as single-track model; this model uses signals from gyro sensor, steering angle and wheel speed encoders. The visual model uses information calculated from the onboard vision system. The sampling sequence diagram is shown in Fig. 1. Obviously, data from visual system and from gyro/encoders cannot be fused directly because of sampling time mismatch. Two solutions can be employed, namely, increase the overall sampling period to fit the longest one, or use multi-rate estimation method. These two methods will be further illustrated in the following sections. The rest of this paper comprises of four sections. In section 2, the combined vehicle and visual model is introduced. The vehicle model is based on traditional two degree of freedom bicycle model and visual model is based on geometry relationship between vehicle and lane. In section 3, experimental vehicle setup and image processing techniques are explained in detail. The experiment vehicle is an in-wheel-motor electric vehicle with Linux-based controller; the vision system consists of a camera and a laptop for real-time image processing; real-time image processing techniques for coordinate mapping, lane detection and location are also explained. In section 4, a multi-rate Kalman filter considering time delay is designed to estimate vehicle lateral position, orientation and lateral velocity; measurement delays caused by image processing are augmented to the system state space equation, and the current states can be estimated with the information one step before; for the multi-rate issue, a switching method for measurement update is adopted, and the estimator can be updated every 1 ms. In section 5, to verify the proposed multi-rate Kalman filter, both simulations and experiments are conducted; the results demonstrate effectiveness of the multi-rate Kalman filter.

2. SYSTEM MODELING

In this section, both vehicle and vision models are explained; to construct state space equations for estimation, the vehicle and vision models are combined as a new system [8-9, 20-21].

2.1. Vehicle Model

Vehicle dynamics are difficult to be described precisely due to its high non-linearity, and for the benefit of implementation, simple linear model is preferable. Vehicle bicycle model, as illustrated in Fig. 2, is widely used in vehicle state estimation and motion control systems. Detailed information can be found in [7].

The governing state space equation for this model is given by (1), where m is vehicle mass; I is the inertia about vehicle vertical axis; V_x is vehicle longitude speed; V_y is vehicle lateral speed; δ_f *is the angle of steering wheel;* V_{cg} is the speed of vehicle CoG (Center of Gravity); β is body slip angle; γ is yaw rate; C_f and C_r are cornering stiffness of front and rear wheel, respectively; l_f and l_r are distance from vehicle mass center to front and rear wheel, respectively; w and v are the process noise and measurement noise matrixes respectively.

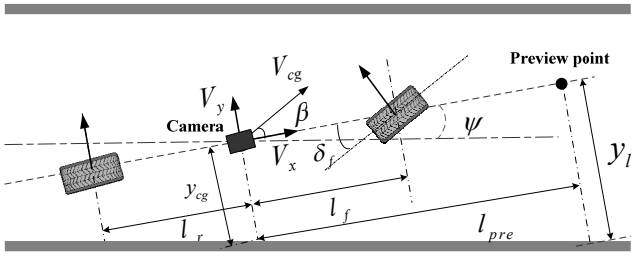

Fig. (2). Combined bicycle model and vision model.

$$\dot{x} = A \cdot x + B \cdot u + w$$
$$y = C \cdot x + v \tag{1}$$

where

$$x = [V_y \quad \gamma]^T, \quad u = \delta_f, \quad y = \gamma,$$
$$A = \begin{bmatrix} -\frac{c_f + c_r}{m V_x} & -V_x - \frac{c_f l_f - c_r l_r}{m V_x} \\ -\frac{c_f l_f - c_r l_r}{I V_x} & -\frac{c_f l_f^2 + c_r l_r^2}{I V_x} \end{bmatrix},$$
$$B = \begin{bmatrix} \frac{c_f}{m} & \frac{c_f l_f}{I} \end{bmatrix}^T, \quad C = \begin{bmatrix} 0 & 1 \end{bmatrix}.$$

2.2. Vision Model

While bicycle model is independent of road reference, vision model contains geometric information by considering vehicle, lane/road together. Vision model is also shown in Fig. 2 together with vehicle bicycle model, and the gray borders are lane makers. l_{pre} is a fixed preview distance needs to be calibrated beforehand. In this model, it is assumed that the vehicle is travelling along a straight road with clear lane markers; the camera is equipped at the CoG of the vehicle and can detect lane boundaries in real time. The lane function can be obtained in the coordinate with camera/vehicle as origin, and then, lateral distance offset, y_l, at the preview point, as well as the heading angle, ψ, can be calculated. y_{cg} is the lateral offset at vehicle CoG.

To derive vision model, ψ and V_y are assumed to be small. Based on the geometric relationships in Fig. 2, y_l can be approximately expressed as (2):

$$y_l = y_{cg} + l_{pre} \cdot \psi \tag{2}$$

The lateral speed at CoG, i.e., the derivative of y_{cg}, is given by (3):

$$\dot{y}_{cg} = V_{cg} \cdot \sin(\beta + \psi)$$
$$= V_y + V_x \cdot \psi \tag{3}$$

By taking the derivative of (2) and substituting (3) into it, equation (4) can be obtained.

$$\dot{y}_l = V_y + l_{pre} \cdot \gamma + V_x \cdot \psi \tag{4}$$

From (4), it can be known that, the derivative of the offset at the preview point, i.e., lateral speed at that point, comprises three parts: the lateral speed of CoG, the components of yaw rate, and the component of longitudinal speed (resulted from vehicle heading angle).

Heading angle ψ can be simply modeled as integration of yaw rate as (5):

$$\dot{\psi} = \gamma \tag{5}$$

It should be noticed that, although curved road is not considered here, models can still be generated in the same manner by modeling curvature with spline function, i.e., this research can be expanded to all the roads with lane markers.

2.3. Combined Vehicle and Vision Model

The combined model can also be given in continuous state space form as (1) with description in (6). The first two states are from bicycle model and the latter two are from the vision model. In the combined model, available system outputs are yaw rate from gyro sensor, vehicle heading angle and lateral offset with reference to lane at the preview point from image processing system. It should be pointed out that the first two states and the second two are updated at different sampling rates.

$$x = [V_y \quad \gamma \quad \psi \quad y_l]^T, \quad u = \delta_f, \quad y = [\gamma \quad \psi \quad y_l]^T,$$

$$A = \begin{bmatrix} -\dfrac{c_f + c_r}{m V_x} & -V - \dfrac{c_f l_f - c_r l_r}{m V_x} & 0 & 0 \\ -\dfrac{c_f l_f - c_r l_r}{I V_x} & -\dfrac{c_f l_f^2 + c_r l_r^2}{I V_x} & 0 & 0 \\ 0 & 1 & 0 & 0 \\ 1 & l_{pre} & V_x & 0 \end{bmatrix},$$

$$B = \begin{bmatrix} \dfrac{c_f}{m} & \dfrac{c_f l_f}{I} & 0 & 0 \end{bmatrix}^T, \quad C = \begin{bmatrix} 0 & 1 & 0 & 0 \\ 0 & 0 & 1 & 0 \\ 0 & 0 & 0 & 1 \end{bmatrix}. \tag{6}$$

Fig. (3). Experimental vehicle.

3. EXPERIMENT SETUP AND IMAGE PROCESSING TECHNIQUES

In this section, the experiment vehicle and sensors are introduced in details; image processing algorithms for lane detection are also explained.

3.1. Experiment Setup

The experimental vehicle used is a single-seat electric vehicle shown in Fig. 3. The prototype is COMS produced by Toyota Auto Body, and it was modified by our lab for capacitor and motion control related researches [18].

Fig. 4 briefly demonstrates the sensors and controller configurations of this vehicle. The vehicle controller is a PC104 embedded computer with ART-Linux operation system, and the program is configured to run at the speed of one millisecond per cycle. In addition to the central computer, four A/D converters and two counter boards are equipped for sensor signal reading. Gyroscope that measures lateral acceleration and yaw rate is installed in the vehicle CoG, and the signals are read by the A/D boards; steering angle and wheel speed encoders are also equipped to send data to the counter board. Besides, to verify the effectiveness of estimation results, a non-contact optical sensor S-400 made by Corrsys-Datron is also equipped for lateral velocity acquisition; since this sensor is installed in front of the vehicle, the measurements are compensated with yaw rate to get the value at vehicle CoG. Vision system includes a camera and an image processing laptop; the camera used is a monocular one produced by Point Gray, and it is installed on the top of the vehicle (assume to be in the CoG) with a tilting angle of 8 degrees and a preview distance of 5.135 m. The frame rate of the camera is set to 30 fps.

Images captured by the camera are grasped by a CARDBUS frame grabber and processed by a laptop with image processing algorithms in Linux environment. The image processing time varies from 8 ms to 25 ms which depends on the CPU load and the incoming images; to make the outputs from image processing program constant, a delay function is implemented. The final outputs from vision system are the estimated ψ and y_l. The two values are sent to vehicle controller via LAN cable using UDP protocol (the time for data transmission can be neglected).

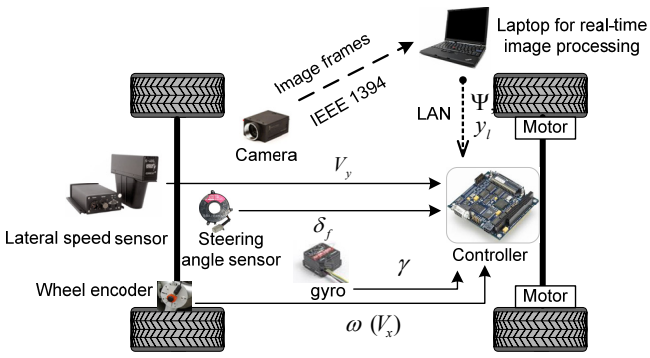

Fig. (4). Sensors setup.

3.2. Image Processing Algorithms

To fuse vision information with signals from other onboard sensors in real-time, on-line image processing is required. In this research, image processing is implemented in C++ with OpenCV library and the library released by Point Grey Research. OpenCV is a free library initially developed by Intel which can facilitate image processing related development. Image processing in this research generally consists of two parts: coordinate mapping and mapped images processing.

Coordinate Mapping. Camera can map the 3-D world onto its 2-D image view; however, this kind of mapping loses important information such as depth and that is why many researches use stereo camera instead of monocular one. For the application of lane capturing, since common roads can be simplified as planar, a monocular camera is fairly enough to correlate pixels of the image with real roads.

Fig. 5 shows the geometric relationships among pinhole camera model, image plane and road plane. In Fig. 5, h is height of camera, f is focal length, θ is camera tilting angle, α_v and α_u are the angle of view in vertical and horizontal axis of image planes, respectively. To find the mapping matrix from image coordinate to road coordinate, one typical method is to calibrate the camera model which is composed of both intrinsic and extrinsic parameters. While this method needs complex calibration, another more straightforward method can get road coordinates from image pixel positions by deriving functions based on geometric relationships [1,10]. For better demonstration, Fig. 5 is reconstructed as Fig. 6 viewing from U axis and V axis of the image plane.

For one arbitrary pixel (u_{pixel}, v_{pixel}) in the image plane, its projection on road plane is given as (x, y). Assume the resolution of image is m by n, equation (7) that mapping road coordinates to pixel coordinates can be derived.

$$u_{pixel} = \frac{m-1}{2} \cdot \left(1 + \frac{h - x \cdot \tan\theta}{h \cdot \tan\theta + x} \cdot \cot\alpha_v\right) + 1$$
$$v_{pixel} = \frac{n-1}{2} \cdot \left(1 - \frac{y}{h \cdot \sin\theta + x \cdot \cos\theta} \cdot \cot\alpha_u\right) + 1 \qquad (7)$$

From (7), it can be noticed that, the row of pixel coordinates only has relationship with x coordinates of the road plane, and the column of pixel coordinate correlate with both x and y coordinate of road plane. After pixel mapping, the generated image represents a bird-eye view of the road.

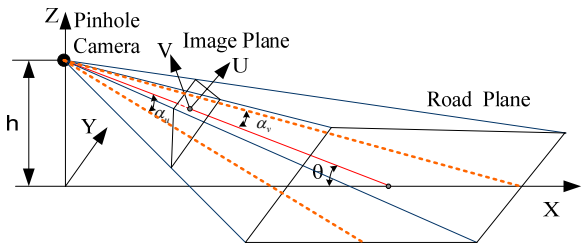

Fig. (5). Geometric relationship between camera and road.

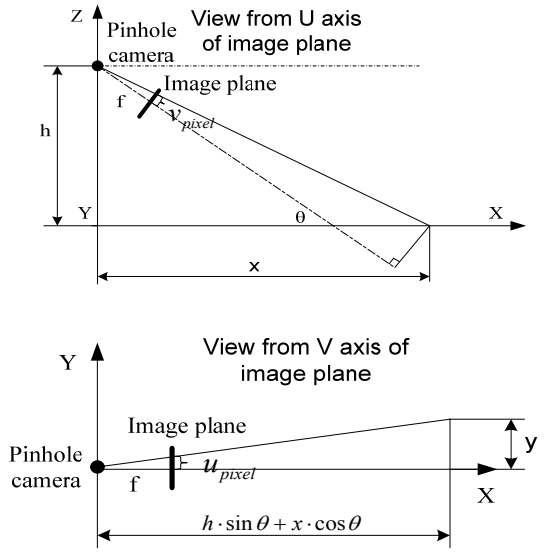

Fig. (6). View from different image plane axis.

Lane Detection and Location. This part consists of two steps: the first step is to extract lane from background, and the second one is to locate the lane position. Results are shown in Fig. 7.

Since images contain noise more or less, it is desirable to smooth the image first. An effective method for image smoothing is Gaussian filter that gives more weight to the current pixel position and then tapers the weights as distance increases according to the Gaussian formula. After pre-processing, the lane detection algorithm can be implemented. One of the most commonly used feature extraction methods is Laplacian; it is a convoluted mask to approximate the second derivative, and to check for zero crossings, i.e., when the resulting value goes from negative to positive or vice versa, the regions of rapid intensity change are highlighted. The above mentioned methods need to be performed in two steps; alternatively, Laplacian of Gaussian (LoG) method can perform the same function in a one step manner. LoG will give zero to the uniform region of the image; wherever a change occurs, the LoG will give a positive response on the darker side and a negative response on the lighter side, and hence the lane can be extracted. In fact, Gaussian derivative offers a simple illustration of steerable filter. Detailed explanations can be found in [2, 11].

Although white lane marker can be extracted from image using the methods outlined above, the positions of white pixels are still unknown. In this study, RANdom SAmple Consensus (RANSAC) algorithm proposed by [12] is adopted to give the solution. This is a re-sampling technique that gives solutions by using the minimum number of required data required for model estimation. Unlike conventional sampling techniques that use as much data as possible to obtain an initial solution, RANSAC randomly selects a smallest data set and solves for the results; and then finds how many data in total fit the model within a given tolerance; if the fitting ratio is large enough, it ends with success, otherwise proceeds to prune outliers [12].

(a) Original image.

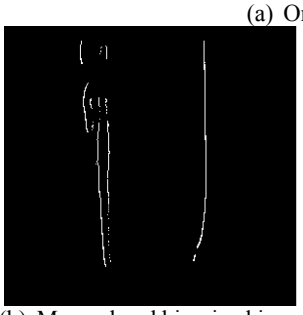

(b) Mapped and binarized image

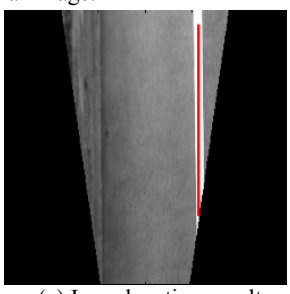

(c) Lane locating result.

Fig. (7). Image processing results.

4. STATE ESTIMATION BASED ON KALMAN FILTER FOR VEHICLE LATERAL CONTROL

Typical continuous state space equation has the form of (1); in this application, vehicle speed, vehicle mass and tire cornering stiffness are not constant, and hence the discretized system matrixes are designed to be time varying as in (8). In (8), T_s is the sampling time, and k is the time step. Fig. 8 describes the general structure of Kalman filter; basically, it consists of time update (also known as prediction) and measurement update (also known as correction) [13]. Kalman filter is a recursive way to get optimal results.

$$x(k+1) = A_d(k)\cdot x(k) + B_d(k)\cdot u(k) + w(k)$$
$$y(k) = C_d(k)\cdot x(k) + v(k) \qquad (8)$$

where

$$A_d(k) = e^{A\cdot Ts},\quad B_d(k) = \int_0^{Ts} e^{A\cdot\tau}\cdot B d\tau,$$
$$C_d(k) = C.$$

Normal discrete Kalman filter has a general structure of (8); however, as measurement delay is introduced by image processing system, the vision output equation can not be expressed using (8), instead, it should has the form of (9).

$$y(k) = C_d(k-n_d)\cdot x(k-n_d) + v(k-n_d) \qquad (9)$$

where T_d is the time delay, and $n_d = T_d/T_s$; T_d is 33 ms, and T_s is 1 ms in this research.

From (9), it is understood that, unlike normal system, the measurements are updated at time k-n_d, but are not available until time k. To compensate such dead time, one patent uses advanced hardware to make the time delay within nanosecond level and hence ignore it [16], but high cost make it impractical. Another patent compensates time delay and other noises by tuning the Kalman gain [17]; yet it is complex to find proper relationship between noise covariance and time delay. Here, an explicit way, augmented-state method, is employed to deal with dead time issue [14]. The basic idea of this method is to include delayed states into the state space equation. First, considering information from camera has a one step delay, (10) can be defined:

$$\overline{\psi}(k+1) = \psi(k),\quad \overline{y}_l(k+1) = y_l(k) \qquad (10)$$

Then, the combined system model in (6) can be discretized to (8) with (10) as additional states, and (11) gives description for the new system.

With the above transformation, delayed vision information is augmented to the original system. As this system is observable, current vision information can be estimated with Kalman filter based on previous ones.

Another problem is, as mentioned before, sampling periods of the system are not consistent; in (11), the first two

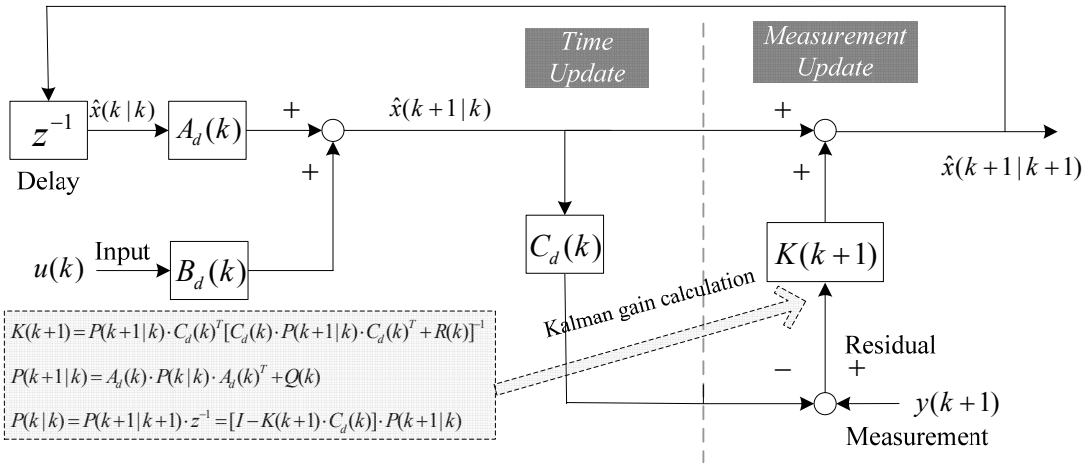

Fig. (8). Block diagram for the principle of Kalman filter.

states and the following four states have different sampling frequencies. Traditional solution is to adapt the whole system sampling time to the longest one and design a single-rate estimator based on the unified sampling time. Here in this paper, multi-rate Kalman filter is constructed to show its advantage over single-rate one.

$$x^a(k) = [V_y(k), \gamma(k), \psi(k), y_l(k), \overline{\psi}(k), \overline{y}_l(k)]^T,$$

$$u(k) = \delta_f(k), \quad y^a(k) = [\gamma(k), \overline{\psi}(k), \overline{y}_l(k)]^T,$$

$$A_d^a(k) = \begin{bmatrix} A_d(k) & O_{4\times 2} \\ O_{2\times 2} & I_{2\times 2} \quad O_{2\times 2} \end{bmatrix}, B_d^a(k) = [B_d(k), 0, 0]^T,$$

$$C_d^a(k) = C_d^a = \begin{bmatrix} 0 & 1 & 0 & 0 & 0 & 0 \\ 0 & 0 & 0 & 0 & 1 & 0 \\ 0 & 0 & 0 & 0 & 0 & 1 \end{bmatrix}. \quad (11)$$

4.1. Single-rate KF based on delay-augmented system

Single-rate Kalman filter simply uses the sampling rate of low speed sensor as basis. In this study, to unify the sampling rate of gyroscope, encoders and camera, system sampling rate is set to adapt camera, i.e., gyroscope and encoders are sampled every 33 ms although they can be updated every 1 ms.

The key factors in Kalman filter design is Kalman gain tuning; the process and measurement noise covariance matrixes determine the gain. After fixing the sampling time, the two matrixes need to be designed for Kalman gain calculation. In (8), w(k) and v(k) are the process noise and measurement noise, respectively, and it is assumed that they are Gaussian with zero-mean, and the covariance matrixes are defined as:

$$Q(k) = E[w(k)w(k)^T]; \quad R(k) = E[v(k)v(k)^T] \quad (12)$$

where Q(k) and R(k) are process and measurement noise covariance matrixes respectively. In selection of Q and R, two points are considered here:

1) To reduce computation burden, these two covariance matrixes are designed to be diagonal, i.e., the noise components are assumed to be independent from each other.
2) Tradeoff needs to be made between Q and R. As the vehicle model contains uncertainty, the corresponding process noise is set to be relatively large; the measurement noise covariance matrixes are tuned based on their own noise properties.

With the above sampling rate adjustment, problems are arisen. For example, measurements from high sampling rate sensors cannot be fully utilized and hence deteriorate the accuracy of measurement update; the estimated vehicle lateral velocity, heading angle and lateral displacement to lane are updated every 33 ms which are not fast enough for general motion control applications [14].

4.2. Multi-rate KF based on delay-augmented system

In [23], George J. Geier *et al.* consider a similar application of the fusion of GPS and other sensors using multi-rate Kalman filter, and it divides the combined system into low-rate and fast-rate ones; [22] also includes multi-rate Kalman filter for fast and low speed sensor combination, but detailed algorithm is not elaborated. In fact, compared with single-rate Kalman filter, the prediction part of Multi-rate one is the same, and the main differences between the two methods are: 1) the continuous state space equations are first discretized using the fast sampling time, in this study, T_s is set to 1 ms; 2) the correction part of Multi-rate Kaman filter needs to be modified during inter-samplings. Assume the camera measurement sampling period is T_c, and during the time intervals of $n \cdot T_c$ (n is an integer), there is no sensor updates from vision system, therefore, the correction of Kalman filter is only based on yaw rate from gyro sensor. Another interpretation can be: pseudo-correction is implemented using estimated visual information (equal to prediction) while real-correction is done with yaw rate feedback. The state estimation equation for multi-rate Kalman filter is shown in (13).

$$\hat{x}^a(k+1|k+1) = \hat{x}^a(k+1|k) + \tilde{K}(k+1) \cdot [\tilde{y}^a(k+1) - C_d^a \cdot \hat{x}^a(k+1|k)] \quad (13)$$

where

$$\tilde{y}^a(k+1) = \begin{cases} [\gamma(k+1), 0, 0)]^T, & if \quad k+1 \neq n \cdot (T_c/T_s), \\ [\gamma(k+1), \overline{\psi}(k+1), \overline{y}_l(k+1))]^T, & if \quad k+1 = n \cdot (T_c/T_s). \end{cases}$$

Kalman gain in (13) changes following $\tilde{P}(k+1|k)$, which is given by the below equation:

$$\tilde{P}(k+1|k) = A_d^a(k) \cdot \tilde{P}(k|k) \cdot A_d^{aT}(k) + Q(k)$$
$$= A_d^a(k) \cdot ([I - \tilde{K}(k) \cdot \tilde{C}_d^a(k)] \cdot \tilde{P}(k|k-1)) \cdot A_d^{aT}(k) + Q(k) \quad (14)$$

where

$$\tilde{C}_d^a(k) = \begin{cases} \begin{bmatrix} 0 & 1 & 0 & 0 & 0 & 0 \\ 0 & 0 & 0 & 0 & 0 & 0 \\ 0 & 0 & 0 & 0 & 0 & 0 \end{bmatrix}, & if \quad k \neq n \cdot (T_c/T_s), \\ \begin{bmatrix} 0 & 1 & 0 & 0 & 0 & 0 \\ 0 & 0 & 0 & 0 & 1 & 0 \\ 0 & 0 & 0 & 0 & 0 & 1 \end{bmatrix}, & if \quad k = n \cdot (T_c/T_s). \end{cases}$$

The above equations illustrate that the Kalman gain is switching between two situations, namely, with and without visual updates. In other words, full measurement updates are done when there are visual feedbacks, and partial measurement updates are done during visual inter-sampling times (the residuals of visual parts are set to 0).

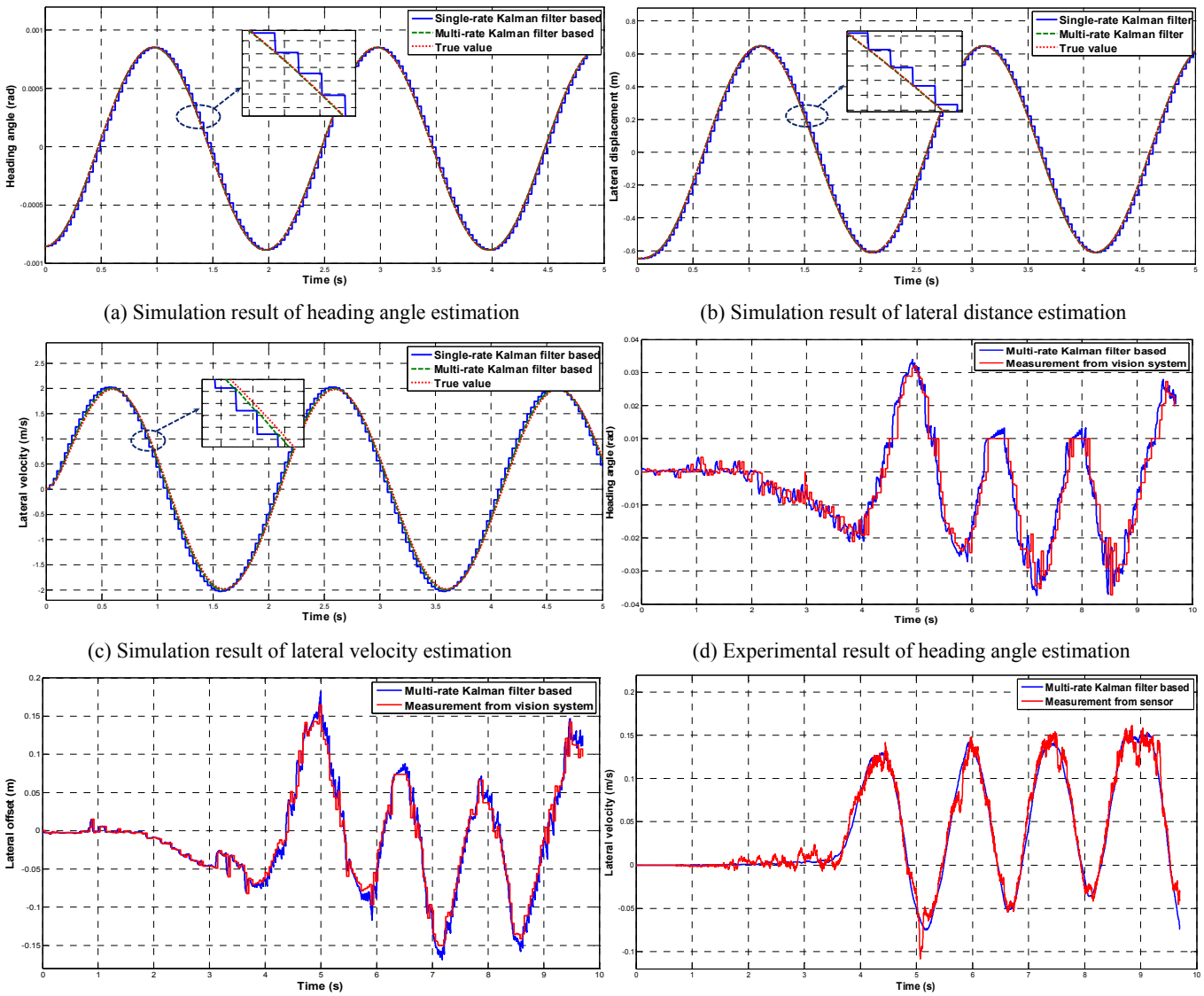

(a) Simulation result of heading angle estimation

(b) Simulation result of lateral distance estimation

(c) Simulation result of lateral velocity estimation

(d) Experimental result of heading angle estimation

(e) Experimental result of lateral distance estimation

(f) Experimental result of lateral velocity estimation

Fig. (7). Simulation and experimental results.

5. SIMULATIONS AND EXPERIMENTS

5.1. Simulation verification

Simulations were conducted to verify the proposed multi-rate Kalman filter. The vehicle was assumed to run at the speed of 30km/h, and a sine steering input was given. To simulate real conditions, model discrepancies were implemented: vehicle plant model and Kalman filter model were made different from each other. For comparison, the combined four states Kalman filter with 33 ms sampling intervals (single-rate KF) is also included in the figures.

Fig. 7 (a) – (c) show the estimation results of heading angle, lateral offset and lateral velocity; it can be observed that the single-rate Kalman filter-based estimation results (blue line) have steps due to the long sampling time; on the other hand, multi-rate Kalman filter-based estimation results (dotted green line) can track true value very well even if the vehicle model is set to be different from Kalman filter model. In other words, multi-rate Kalman filter has higher accuracy compared with the single-rate one; from the viewpoint of control, the open-loop stability margin is increased by using multi-rate Kalman filter.

5.2. Experiment verification

Experiments were conducted with the experimental electric vehicle introduced in section 3. The vehicle was given a sine steering input on a road with lane markers, and the vehicle speed varied from 10 km/h to 20 km/h. Vision system worked in real-time for lane detection.

As true vehicle model can not be known precisely, the Kalman filter model contains parameter mismatches. Fig. 7 (d) – (e) give comparison results of multi-rate Kalman filter-based estimations and sensor measurements. Lateral distance and heading angle measurements come from vision system, and the initial measurements contain noises; in some parts of the visual information, out-of-view issues occurred. With the proposed multi-rate Kalman filter, the two signals are smoothed, and the out-of-view parts are compensated.

Fig. 7 (e) is the experimental result of lateral velocity, and this is an unknown state in (11). As can be observed, the multi-rate Kalman filter-based estimation result matches sensor measurement very well.

5. CONCLUSION

In this paper, a combined vehicle and visual model is explained; real-time image processing techniques based on OpenCV library for lane detection and location are introduced; experimental setups are introduced in details; vehicle lateral states estimator based on multi-rate Kalman filters is designed. Both simulations and experiments are performed to demonstrate the effectiveness of the multi-rate Kalman filter.

6. CURRENT AND FUTURE DEVELOPMENTS

The works related to this research can generally be divided into three parts: image processing for lane detection; estimation for vehicle states; vehicle lateral control. Based on these three aspects, future developments of this study can concentrate on:

1) Robust image processing for lane detection. Lane detection using image processing system has been studied for quite a long time; however, due to illumination change and clarity of lane, perfect lane detection is still not possible. Therefore, robust image processing methods need to be investigated for lane detection with high fidelity.

2) Enhanced vehicle lateral states estimation. In addition to traditional single-rate estimator, multi-rate estimator with better performance is developed in this paper; on the other hand, the proposed multi-rate Kalman filter can be further improved with inter-sample estimation (estimate the measurement updates during inter-samples).

3) Enhanced vehicle lateral control. As this paper gives a better vehicle states estimation method compared with previous literatures/patents, vehicle lateral control applications such as lane keeping and automatic driving system can be implemented with the proposed estimator. Moreover, as new vehicle structure such as in-wheel-motor driving system becomes more and more mature, vehicle lateral control using in-wheel-motors as actuators can be promising with the proposed multi-rate estimator.

CONFLICT OF INTEREST

The authors have no conflicts of interest to declare.

REFERENCES

[1] Massimo Bertozzi, Alberto Broggi, "GOLD: A Parallel Real-Time Stereo Vision System for Generic Obstacle and Lane Detection", *IEEE Trans. on Image Processing*, Vol. 7, No. 1, Jan. 1998.

[2] McCall, J.C., Trivedi, M.M., "Video-based lane estimation and tracking for driver assistance: survey, system, and evaluation", *IEEE Trans. on ITS*, Vol. 7, No. 1, Mar. 2006.

[3] Timothy W. Kaufmann, Farhad Bolourchi, "*Systems, methods and computer program products for lane change detection and handling of lane keeping torque*", US 7885730 B2, 2008.

[4] Toru Saito, Shinya Kudo, Hjime Oyama, "*Lane keeping assistance equipment for automotive vehicles*". US 7890231, 2011.

[5] Chenming Zhao, Weidong Xiang, Richardson, P., "Vehicle Lateral Control and Yaw Stability Control through Differential Braking", *IEEE ISIE*, 2006, pp. 384 - 389.

[6] Yoichi Hori, "Future Vehicle driven by Electricity and Control - Research on 4 Wheel Motored 'UOT March II'", *IEEE Trans. on Industrial Electronics*, Vol.51, No.5, pp.954-962, 2004.10.

[7] C. Geng, L. Mostefai, M. Denai and Y. Hori, "Direct Yaw Moment Control of an In-Wheel-Motored Electric Vehicle Based on Body Slip Angle Fuzzy Observer", *IEEE Transactions on Industrial Electronics*, Vol.56, No.5, 2009.

[8] Marino, R., Scalzi, S., Orlando, G., and Netto, M., "A nested PID steering control for lane keeping in vision based autonomous vehicles", *American Control Conference*, St. Louis, 2009, pp: 2885-2890.

[9] Kosecka, J., Blasi, R., Taylor, C.J., and Malik, J., "Vision-based lateral control of vehicles", ITSC '97., IEEE Conference on, Boston, pp: 900-905.

[10] Muad, A.M. Hussain, A. Samad, S.A. Mustaffa, M.M. Majlis, B.Y., "Implementation of inverse perspective mapping algorithm for the development of an automatic lane tracking system", *TENCON 2004*, Vol. 1, 2004, pp. 207-210.

[11] Freeman, W.T., Adelson, E.H., "The design and use of steerable filters" *Pattern Analysis and Machine Intelligence, IEEE Transactions on*, Sept. 1991, pp. 891-906.

[12] M.A. Fischler and R.C. Bolles. "Random sample consensus: A paradigm for model fitting with applications to image analysis and automated cartography", *Comm. of the ACM*, pp. 381–395.

[13] M. S. Grewal and A. P. Andrews, Kalman Filtering: Theory and Practice Using MATLAB, Wiley Online Library, 2001.

[14] Dejun Yin, Yoichi Hori, "A Novel Traction Control for EV Based on Maximum Transmissible Torque Estimation", *IEEE Trans. on Industrial Electronics*, Vol. 56, No.6, 2009.

[15] L. Wang, L. Fang, Y. Zhao, "*Vehicle all-round looking and lane detection alarming system*", CN 201780482, 2011.

[16] Uenuma Kenya, Satoh Shigeki, Furusho Hiroyuki, Shimakage Masayasu, Mouri Hiroshi, "*Lane-following system by detection of lane marking*", US 6580986, 2003.

[17] B. Bhowmick, A. Sinharay, A. Pal, S. Bhadra, "Automatic detection of moving object by using stereo vision technique", WO 2012001709, 2012.

[18] K. Kawashima, T. Uchida, and Y. Hori, "Manufacturing of Small Electric Vehicle driven only by Electric Double Layer Capacitors for Easy Experiment of Vehicle Motion Control", *Electric Vehicle Symposium 21*, 2005.4.

[19] G. Bradski, A. Kaehler, "Learning OpenCV: Computer Vision with the OpenCV Library", *O'Reilly,Cambridge*, MA, 2008.

[20] Y. Wang, P. Kotchapansompote, H. Fujimoto and Y. Hori, "Multi-rate estimation for vehicle body slip angle using onboard vision system", SNU-UT Joint Seminar 2011, Kashiwa.

[21] Y. Wang, B.M. Nguyen, P. Kotchapansompote, H. Fujimoto, Y. Hori, "Vision-based Vehicle Body Slip Angle Estimation with Multi-rate Kalman Filter considering Time Delay", ISIE 2012, Hangzhou, China.

[22] Clark E. Cohen, Robert W. Brumley, Mark L. Psiaki, Gregory M. Gutt, William J. Bencze, Brent M. Ledvina, Barton G. Ferrell, David A. Whelan, "Methods and apparatus for a navigation system with reduced susceptibility to interference and jamming", US 7372400, 2008.

[23] George J. Geier, Thomas M. King, Ravikiran Nory, Xiang Yuan, "Frequency error tracking in satellite positioning system receivers", US 7061425, 2006.